

Thick disks and halos of spiral galaxies M 81, NGC 55 and NGC 300. [★]

Tikhonov N.A.^{1,2}, Galazutdinova O.A.^{1,2}, Drozdovsky I.O.^{3,4}

¹ Special Astrophysical Observatory, Russian Academy of Sciences, N.Arkhыз,
KChR, 369167, Russia

² Isaac Newton Institute of Chile, SAO Branch, Russia

³ Spitzer Science Center, Caltech, MC 220-6, Pasadena, CA 91125, USA

⁴ Astronomical Institute, St.Petersburg University, 198504, Russia

Received June 5, 2019

Abstract. By using images from the HST/WFPC2/ACS archive, we have analyzed the spatial distribution of the AGB and RGB stars along the galactocentric radius of nearby spiral galaxies M 81, NGC 300 and NGC 55. Examining color-magnitude diagrams and stellar luminosity functions, we gauge the stellar contents of the surroundings of three galaxies. The red giant population (RGB) identified at large galactocentric radii yields a distance of 3.85 ± 0.08 Mpc for M 81, 2.12 ± 0.10 Mpc for NGC 55, and 2.00 ± 0.13 Mpc for NGC 300, and a mean stellar metallicity of -0.65 , -1.25 , and -0.87 . We find that there are two number density gradients of RGB stars along the radius, which correspond to the thick disk and halo components of the galaxies. We confirm the presence of metallicity gradient of evolved stars at these galaxies, based on the systematic changes of the color distribution of red giant stars. These results imply that thick disk might be a general feature of the spiral galaxies, and endorse a further investigation of the outer stellar edges of nearby spirals, which is critical in constraining the origin and evolution of galaxies.

Key words. Galaxies: individual: M 81, NGC 55 and NGC 300 — galaxies: stellar content — galaxies: photometry — galaxies: structure

1. Introduction

The fossil record of galaxy formation and evolution is imprinted on the spatial distribution, ages and metallicities of galactic stellar populations. The properties of the outer parts of galaxies are very sensitive to both galaxy star formation history and the nature of the intergalactic medium.

The various studies of the nearest spiral galaxies (Milky Way, M31, M33) revealed their similar structure: bulge, thin and thick disks, and halo (van der Marel, 2001; Zocalli et al., 2002; Sarajedini & van Duyne, 2001; Pritchet & van der Bergh, 1988; Belazzini et al., 2003; Guilandre et al., 1998; Brown et al., 2003; Zucker et al., 2004). Aside from the spatial distribution law and kinematics, stars from each of this subsystem share the common star formation history retaining considerable age and chemical information (Vallenary et al., 2000; Prochaska et al., 2000; Chiba & Beers, 2000; Zoccali et al., 2002; Williams, 2002; Sarajedini et al., 2000; Brewer et al., 2003).

The majority of the investigations concentrated predominantly on the central parts of these galaxies, biased towards high surface brightness star forming regions. In recent years, wide-field observations of the nearest spirals have shown that they are substantially more extended than previously thought. The information on the actual origin of these outer regions is scarce, and has been a matter of debates. Today, we know that most of these extended, elusive stellar components are predominantly evolved, but whether this is a true single burst ancient stellar population, with little or no intermediate-age component has not yet been established. By ‘population’, we mean here an ensemble of stars that share a coherent history.

Tests of formation scenarios have centered on two extreme viewpoints — (1) the monolithic collapse model for the halo (Eggen et al., 1962) together with internal chemodynamical evolution for the thick disk (e.g. Burkert et al., 1992), and (2) the accretion model for both, the halo (Searle & Zinh, 1978) and the thick disk (Carney et al., 1989; Gilmore, Wyse and Norris 2002). In view of merging Sagittarius dwarf galaxy with Milky Way (Ibata, Gilmore & Irwin 1995), and the predictions of cold dark matter (CDM) cosmological models for hierarchical galaxy formation from large number of mergers, the accretion origin of the thick disk and halo is especially relevant. On other hand, there are evidences for the significant difference between chemical abundance pattern of the Milky Way’s halo stars and the remaining satellite galaxies, implying of a different evolution history (Brewer & Carner, 2004; Venn et al., 2004).

It is rather easier to separate the spherical bulge and exponential thin disk components based on their distinctive surface brightness profiles (Kent, 1985; Byun & Freeman, 1995;

* Based on observations with the NASA/ESA Hubble Space Telescope, obtained at the Space Telescope Science Institute, which is operated by the Association of Universities for Research in Astronomy, Inc., under NASA contract NAS 5-26555.

Bagget et al., 1998; Prieto et al., 2001), than the thick disk from halo, due to an extremely low surface brightness of these galaxy components, typically below the $\mu_V \sim 26 \text{ mag}/\square''$. While some of the recent studies of the outer regions of spiral galaxies was based on the multicolor surface photometry, the successful detection is possible either in the nearest galaxies or in the galaxies with a bright and extended thick disk/halo (e.g. Harris & Harris, 2001). For example, Dalcanton & Bernstein (2002) analyzed the sample of 47 edge-on spiral galaxies and have found a presence of the thick disk in 90% of them, based on the results of multicolor surface photometry. Star number counts are more optimal for studying galactic outskirts due to their extremely low surface brightness and the possibility to eliminate young stars from the thin disk and background objects.

Our goal here is to extend the study of stellar thick disks and halos over a set of spiral galaxies outside the Local group. M 81, NGC 55 and NGC 300 may provide a contrasting environment, and opportunity to examine the stellar populations on larger galactic scales. In particular we address the following two issues: the spatial distribution of different stellar populations in the outskirts of spiral galaxies and the metallicity gradient of these populations. The brief information about the galaxies is given in Table 1. Each of these object has the HST images of several fields, situated in various distances from center. The high spatial resolution of HST allows us to perform single-star photometry even in crowded fields. The availability of images on various galactocentric distances allows us to reconstruct the behavior of stellar density along a galactocentric radius. Since thick disks and halo consists of old stars - red giants and, to a lesser degree, AGB stars - therefore only these stars were in our consideration. The young stellar populations, located at thin disks of galaxies, have been studied in details (Zickgraf et al., 1990; Georgiev et al., 1992a,b; Pritchet et al., 1987; Kizskurno-Koziej, 1988; Pierre & Azzopardi, 1988) and are not considered in the current work.

A brief description of the target galaxies and justification for their selection is given in Section 2, followed in Section 3 by a description of the HST data and reduction techniques. Our results are discussed in Section 4 and summarized in Section 5.

2. The galaxies

2.1. M 81

M 81 is the gravitationally dominant member of its group, consisting of about 30 various types of galaxies (Börngen et al. 1982, 1984; Karachentseva et al., 1985). The galaxy is a suitable object for this study because of its close distance, $D = 3.6 \text{ Mpc}$ (Freedman et al., 2001); and small inclination, which provide an opportunity to study the geometry of the stellar structures across the disk plane.

While young stellar populations of M 81, populating mainly its spiral arms, have been previously studied in numerous investigations, little is known about the galaxy periphery.

Its optical surface brightness profile have been traced out to $\mu_V \sim 25 - 26^m/\square''$ limiting isophotes (Tenjes et al., 1998), corresponding to major and minor axis diameters of about $24' \times 14'$. The surface brightness color index is unreliable indicator of different stellar populations. For example, the AGB and RGB stars, while differ in age, may have almost the same color, and therefore it become difficult to determine reliably the age of the observed structures. Since spectral observations of outer regions are impossible due to the low surface brightness, the stellar photometry is the only method for the study the outer stellar structures.

The radio observations of M 81 revealed hydrogen bridges from M 81 to the neighboring galaxies M 82, NGC 2976, and NGC 3077 (van der Hulst, 1978; Appleton et al., 1981; Yun et al., 1994; Westpfahl et al., 1999; Boyce et al., 2001). The long gaseous filaments, generated by galaxy interactions, are gravitationally unstable and they might be fragmented to isolated systems, forming young Tidal Dwarf Galaxies (TDG) (Barnes & Hernquist, 1992; Elmegreen et al., 1993; Duc et al., 1998; Weilbacher, 2002). TDG candidates are discovered in many interacting pair of galaxies (Deeg et al., 1998; Hunsberger et al., 1996). It have been suggested that dwarf galaxies Ho IX, Garland, BK3N, observed within the hydrogen bridges of M 81, may be some of them (Miller, 1995; Flynn et al., 1999; Boyce et al., 2001). By comparing the results of observations with theoretical isochrones, Sakai & Madore (2001) concluded that the age of young stars in Garland is less than 150 Myr. The star formation history of Ho IX, Garland and BK3N, estimated from the single-star photometry of the HST images (Makarova et al., 2002), confirm the intensive star formation in these galaxies on the time scale of 50-150 Myrs. In their study, however, the possible presence of the outer stars from the neighboring M 81 and NGC 3077 have not been considered. The underlying stellar population with ages more than 1 Gyr, observed by Makarova et al. (2002), is actually may be related to the outskirts of M 81 and/or NGC 3077 than to the underlying stellar population of the studied galaxies.

2.2. NGC 55

The spiral SB(s)m galaxy NGC 55 (Fig.2) is a member of the Sculptor group, consisting of approximately 30 galaxies (Cote et al., 1997; Jerjen et al., 2000). Since the galaxy is seen almost edge-on (see Table 1), it is a convenient object for studying the extend of the thick disk and halo perpendicularly to a disc plane.

We have measured the distance to NGC 55 as 2.1 Mpc that differs from the previous estimations by Graham (1982) of $D = 1.45$ Mpc, based on the tip of the red giant branch method (TRGB); and Pritchett et al. (1987) of $D = 1.34$ Mpc, using photometry of Carbon stars. We estimated the distance to NGC 55 as 2.1 Mpc that differs considerably from those results.

The galaxy's neutral hydrogen disk has an angular size of about $45 \times 12'$ (Puche et al., 1991). It is plausible that part of this gas was driven out by the stellar winds during galaxy evolution. It has been also reported detection of a large diffused structure which extends up to about 3 kpc above the disk of NGC 55 seen in Chandra X-ray, VLT $H\alpha$, and Spitzer FIR emission (Oshima et al., 2002; Otte & Dettman, 1999; Engelbracht et al., 2004).

2.3. NGC 300

The spiral galaxy SA(s)d (NED) NGC 300 is another member of the Sculptor group. Graham (1982) assumed that NGC 300 located on the same distance as NGC 55, i.e. $D = 1.45$ Mpc. Later, Graham (1984) estimated the distance $D = 1.65$ Mpc using photometry of Cepheids. The recent accepted distance is $D = 2.1$ Mpc, based also on the Cepheids photometry (Freedman et al., 1992). Butler, Martinez-Delgado, & Brandner (2004) determined the distance modulus estimate based on the TRGB method ($m - M$) = 26.56 in good agreement with the Cepheid distance determined by Freedman et al. (1992). We confirmed their results independently from the I -band TRGB method when we estimated a distance of $(m - M) = 26.50$ based on a similar set of HST data.

The low inclination of NGC 300 (see Table 1) allows us to investigate both central part of the galaxy and its periphery. NGC 300 has a large hydrogen disk, $55' \times 50'$ (Rogstad et al., 1979; Puche et al., 1990) – it extended far more than visual part of the galaxy. The central part of NGC 300 is studied in detail, like for most of other galaxies, but the information about outer stellar population is scarce. The brightest stars of NGC 300 have been studied spectroscopically for the identification of blue supergiants and determining a metallicity gradient along the galaxy disk (Bresolin et al., 2002). Using the RGB stars of the disk or the halo we are able to track the surface number density and metallicity gradients for the fainter and at least a Gyr elder stellar populations.

3. Observations, data reductions and analysis.

3.1. HST WFPC2 and ACS/WFC observations

To study the resolved stellar population of galaxies, we obtained all available HST archival images of M 81 (9 WFPC2 fields), 3 WFPC2 and 6 ACS/WFC regions of NGC 300 and 3 WFPC2 fields around NGC 55. Digital Sky Survey images of these galaxies and WFPC2 & WFC footprints are shown in Fig. 1,2,3. The observational data are listed in Table 2, where R is the angular galactocentric distance of the observed field in arcminutes, ID is the HST program number and N_{stars} is the number of detected stars. Images were reprocessed through the standard WFPC2 and ACS STScI pipeline, as described by Holtzman et al. (1995a). After removing cosmic rays, we performed single-star photometry with

packages DAOPHOT and ALLSTAR in MIDAS (Stetson, 1994). These programs use an automatic star-finding algorithm, followed by measurements of their magnitudes via point-spread-function (PSF) fitting that is constructed from the isolated 'PSF-stars'. For the WFPC2 data we applied the aperture correction from the 1.5 pixel radius aperture to the standard $0''.5$ radius aperture size for the WFPC2 photometric system using the PSF-stars. The F555W, F606W and F814W instrumental magnitudes has been transformed to standard magnitudes in the Kron-Cousins system using the prescriptions of Holtzman et al. (1995b). For the ACS/WFC we derived an aperture correction to the $0''.5$ (10 pixels) standard aperture from the data. The final ACS photometry uses the latest available photometric zero-points in the *HST* Vegamag system as provided by the STScI ACS team (Instrument Science Report ACS 2004-08). The background galaxies, unresolved blends and stars contaminated by cosmetic CCD blemishes were eliminated from the final lists, using their characteristic ALLSTAR parameters, $|SHARP| > 0.3$, $|CHI| > 1.2$ (Stetson, 1994).

3.2. Method and star selection.

The primary goal of this study is to determine the basic morphological and chemical properties of the outer stellar surroundings of the target spiral galaxies. Using color-magnitude diagrams and stellar luminosity functions, we separated different stellar populations and analyzed their spatial distribution. We have compared stellar population characteristics of available fields differentially, avoiding some the complications of comparisons with stellar evolution models. Because the RGB loci for old stars are far more sensitive to metallicity than age, we use them to construct a first-order metallicity distribution functions, neglecting some known age-metallicity degeneracy. The spectroscopy of individual thick disk/halo stars will be needed to break the age-metallicity degeneracy inherent to broad-band RGB colors.

Since the purpose of our research is to define change of the stellar number density with increasing galactocentric distance, we should be sure that various selection effects do not affect considerably the final results or at least that their influence can be corrected. For this the following considerations were taken into account:

(i) All the data for this investigation were retrieved from the HST archive and was obtained as a part of different programs. While this allowed us to collect far more data than would be possible in a single primary program, it limited our research. The data differ in exposure time, affecting the total number of resolved point sources. To minimize the influence of different depth on number of detected stars we established a limiting luminosity threshold from the field with shortest exposure time. The single threshold was used to exclude fainter stars from all fields. This limit was established to be a magnitude brighter than the photometric limiting depth, corresponded to the detection completeness

level of $\sim 40\%$ derived from the artificial star trials. We also restricted our work to observations in $F555W$, $F606W$, and $F814W$. Being aware of different band-width of $F606W$ and $F555W$ we intercompare the derived $V - I$ color (from $F606W - F814W$ and $F555W - F814W$) of RGB stars at close galactocentric distances.

(ii) By removing the cosmic ray traces, we decreased their influence on the stellar counts. This step is important in sparse fields of halo, where the number of residual cosmic rays is comparable to the number of faint stars. The limiting depth selection of stars at the level of a magnitude above the photometry limit, also allow to minimize the possible influence of cleaning for cosmic rays on the star counting. As a result, the reduced number of stars increases the statistical fluctuations, but the number density of stars are less influenced by residual traces of cosmic rays.

(iii) The completeness of stars detection, especially at faint levels, is also effected by crowding of stars, which increases towards galaxy center. We excluded from our analysis the central galactic areas due to difficulties with the separation of evolved bulge stellar populations from the thick disk and halo ones. The artificial star trials have been used to correct the number density for the incompleteness.

(iv) Due to some inclination of the observed galaxies, it is important also to correct the measured stellar counts for the azimuthal position of the field. While changes in thickness of the disk might influence the results, it should not significantly change the radial gradients.

(v) Another concern here is our ability to distinguish by multi-color photometry alone a grouping of stars in the thick disk/halo from the plethora of stars found in the galaxy's enveloping thin disk. Can we separate the AGB and RGB stars between these two disks? For the high-inclination systems, as NGC 55, this selection is evident, since at large distances from disk plane the thick disk is a dominant contributor of stars. Several studies have shown that thick disk/halo stars are uniformly elder and more metal poor than thin disk ones (Gilmore & Wyse 1985; Carney et al. 1989). If the thick disk stars are uniformly old, then any star whose life expectancy is brief will necessary belong to the thin disk, regardless of its kinematics or metallicity. By sorting stars on the different groups according to their life expectancies, we can assign probable membership of stars to the thin disk or thick-disk populations. The measurements of the stellar density along galaxy radius on the border of the thin disk may clarify this question. In one of our cases (see section 4.3), the density of RGB stars decreases monotonously and does not uncover the border of the thin disk.

We have not considered the AGB stars as a good tracer of a thick disk. The relative density of the AGB stars in comparison with RGB stars are lower and their evolutionary status is less certain. Although, sometimes they are a good indicator of the edge of the thin disk.

4. Results

4.1. CM Diagrams of M 81, NGC 55 and NGC 300.

The median number of stars detected in both the *F814W* and *F555W/F606W* filters in the WFPC2 fields is about 5,000, and $\sim 10,000$ in the ACS fields for NGC 300 (see Table 2). The results of stellar photometry are presented on the CMDs (Fig. 4 and 5). The features of these diagrams resemble those of spiral galaxies. All the CMDs are characterized by a noticeable red plume, while strength of the blue plum varies a lot. The spatial variations are apparent from the varying strengths of the blue and red plumes, and show systematic dependence from galactocentric distance of the field. The CMDs of the circumnuclear fields show evidence of blue and red supergiants, main-sequence stars, and blue-loop stars. The outer-field stellar populations are dominated by the “red tangle”, which contains the red giant branch. Above this tangle a population of asymptotic giant branch (AGB) and red supergiant stars (SRG) can be seen. The dashed line in all the presented CMDs indicates the position of the tip of the red giant branch (TRGB).

4.2. Distances

The errors in distances of investigated galaxies do not significantly affect our major goal, constraining the relative stellar density distribution. In the context of distance verification, however, it is a good opportunity to compare the the tip red giant branch (TRGB) estimations with other methods. The absolute magnitude of the TRGB gives an estimate of distance with precision and accuracy similar to that of the Cepheid method, $\leq 10\%$ (Lee et al., 1993; Bellazzini et al. 2001). It is slightly dependent on metallicity. A metallicity determination is made to correct for this dependence. The *I*-band TRGB method has been successfully applied to a wide range of dwarf galaxies, using both ground-based and HST photometry.

To the author’s knowledge, this is a first measurement of M 81 and NGC 55 distances based on this method. As it was shown in several studies the distance estimated with the Cepheids method can significantly differ from the TRGB and other methods. For example, in case of well studied M 33 the disagreement between two methods is $\sim 0^m.3$ in distance modulus, which is a large value for the galaxy located in the Local Group (Lee et al. 2002; Kim et al. 2002). Therefore, it is valuable to compare different distance indicators in other galaxies to reveal possible reasons of such dispersion.

In order to estimate distances, we have used one or several fields for each galaxy, avoiding star formation regions with bright supergiants. We preferred fields with large number of red giant to decrease statistical error of TRGB method. These fields are - S2, S3, S4, S5, S6 for M 81 (Fig.1), S3 for NGC 55 (Fig.2) and S1 for NGC 300 (Fig.3). CM diagrams of these fields are shown in Figs. 4 and 5. A typical samples of incompleteness

of such fields are shown in Figs. 6 and 7. The stellar luminosity function of such field has a gap which corresponds to the tip of red giant branch (TRGB)(see Fig.8). Using the method of Lee et al. (1993), we have estimated distances to galaxies and mean metallicity of red giants. The extinction coefficients of all galaxies were taken from the study of Schlegel et al. (1998).

We have obtained following results for the different fields around M 81: field S2 $(m - M) = 27.89 \pm 0.10$, field S3 $-(m - M) = 27.89 \pm 0.10$, field S4 $-(m - M) = 27.95 \pm 0.10$, field S5 $-(m - M) = 27.95 \pm 0.10$ and field S6 $-(m - M) = 27.95 \pm 0.10$. The metallicity of inner fields (S2, S3, S5, S6) varies from -0.6 to -0.7 , while the metallicity of outer field S4 is $[Fe/H] = -0.77$. We estimated mean distance modulus for M 81 as $(m - M) = 27.93 \pm 0.04$ (that corresponds to $D = 3.85 \pm 0.08$ Mpc) which is very close to the mean distance of 16 dwarf galaxies of the group, $(m - M) = 27^m9$, determined with TRGB method (Caldwell et al. 1998, Karachentsev et al. 2002). This indicates that M 81 is near the center of the group and there is no asymmetry of spatial distribution of galaxies in the group.

The Cepheids distance estimation for M 81 have been derived by Freedman et al. (2001), corresponding to distance modulus of $(m - M) = 27.75 \pm 0.08$. The new longer distance derived in this paper, $\Delta(m - M) = 0^m18$, are above the estimated errors and not correlated with metal content.

For NGC 55 (field S3) we estimated following values: $(m - M) = 26.64 \pm 0.10$, $D = 2.12 \pm 0.10$ Mpc and $[Fe/H] = -1.25$. Our distance estimation differs essentially from the value of Puche et al. (1991) $D = 1.6$ Mpc but it is in accordance with the suggestion of Graham (1982) that galaxies NGC 55 and NGC 300 are at the same distance.

For NGC 300 (field S1) we obtained following results: $(m - M) = 26.50 \pm 0.15$, $D = 2.00 \pm 0.13$ Mpc, and $[Fe/H] = -0.87$. The distance is very similar to the result of Freedman et al. (2001), $(m - M) = 26.53 \pm 0.07$ ($D = 2.02$ Mpc), based on the Cepheid photometry.

4.3. Metallicity gradient of the RGB stars along galactocentric radius.

The metallicity gradients along the galactocentric radius have been established in the Galaxy and other nearby spiral galaxies, on the basis of the spectroscopy of stellar clusters (e.g., Friel & Janes, 1993; Rolleston et al., 2000) and HII regions (e.g., Shaver et al., 1983; Marquez et al., 2002). However, only few galaxies are close enough to perform metallicity measurements from spectra of evolved stellar populations (red-giants) due to their low luminosity (Reitzel & Guhathakurta, 2002). The idea to use the $V - I$ color of the RGB stars come from its much greater sensitivity to metallicity than is has to age, making it a good stellar metallicity indicator (although there is some degeneracy). The advantage of this method is that red giants can be seen on relatively large distances from

galactic center, where a surface brightness is very low and spectral methods are below the sensitivity limits.

Among the selected galaxies the most apparent metallicity-age gradient is observed in M 81, based on the comparison of the mean colors of the RGB locus from different fields. The mean metallicity of red giants in the S2, S3, S5, S6 fields is $[Fe/H] = -0.65 \pm 0.03$. For the field S4, which has a larger galactocentric distance (Fig. 1) the mean RGB metallicity is $[Fe/H] = -0.77$.

The metallicity gradient of the galaxy NGC 300 in the fields S1 and F4 is well seen in Fig. 9. The maximum of the stellar color distribution (mode of the distribution) traces the RGB position. This maximum is changed from $(V - I) = 1.40$ to $(V - I) = 1.48$ along the galactocentric radius, conforming with metallicity increase of the RGB stars in the assumption of their uniform prevailing age. We investigated the color of RGB stars throughout the thin disk of NGC 300 using the ACS/WFC and WFPC2 images and found that there is a presence of a color gradient of RGB stars at the edge of thin disk (fields S1 and F4) and near the center of the galaxy (Fig.9). The decreasing of the color index to the center of galaxy may be a summary effect of the age and metallicity of red giants. Thus the number of the red giants with a lower metallicity or with less average age increases near the center of galaxy. At the edge of the galaxy the color index decrease can be explained only by the decrease of the metallicity along radius, because the age of red giants can not decrease at the periphery without signs of star formation processes. The color index and then the metallicity of the red giants along thin disk body has no considerable changes.

The measurements of the edge-on galaxy NGC 55, demonstrated a very low metallicity gradient. This probably due to the fact, that measurements have been performed along the small axis of the galaxy, but not along the radius.

4.4. Surface density of AGB and RGB stars in galaxies.

The main goal of the this paper is to study of stellar distribution around spiral galaxies. Earlier, on basis of the study of 16 irregular dwarf galaxies, we discovered that red giants form a thick disk around each galaxy. The size of such disk is 2-3 times larger than those of visible part of the galaxy (Tikhonov, 2002). We did not detect stars that belong to the galaxy beyond of these disks. At the same time, our study of a more luminous irregular galaxy IC10 demonstrated that it has an extended disk (Tikhonov, 1999) and a more extended halo behind the sharp edge of this disk (Tikhonov, 2002; Drozdovsky et al., 2002). It is interesting, that the red giants of IC 10's disk and halo demonstrate different gradients of stellar density. A sharp border between thick disk and the halo is detected in galaxy M 33 (Guillandre et al., 1998). However, the authors did not measure the density gradients of red giants in the thick disk and the halo. The surface distribution of various

objects in M 31 was investigated by Ferguson et al. (2002) on the basis of wide field images. It was discovered that the stellar density as well as the mean metallicity vary along the galaxy radius.

Using only the archival data limited our ability to analyze the true extend of the outer stellar structures. Unable to plan the mapping of the the galaxy outskirts in a manner that optimized the science return, we make an assumption of an axial symmetry of the disk and halo components, ignoring possible tidal deformation. Since galaxies have an inclination to the line of sight, we calculated the distance from the investigated area to the galactic center with the following equation:

$$Radius = \sqrt{(D_a)^2 + (D_b/\cos A)^2}, \quad (1)$$

where D_a is a projection of the seen distance from the investigated area to the galaxy center on the large galaxy axis, D_b is the same projection on the small axis of the galaxy, and A is the galaxy inclination angle to the line of site. In this way, distances for all fields of M 81 were calculated and the distribution of stars along the galaxy radius was constructed. However, before constructing the distribution, we performed a selection of objects and stars number correction for the incompleteness of sample as described in section 2.2.c.

4.5. M 81.

The HST/WFPC2 archive contains a plethora of data located at different areas around M 81, from the central spiral arms to the galaxy outskirts (see Figure 1). On the central fields, we avoided to use regions of the intense star-formation by masking them out, since star counts become heavily contaminated by young and intermediate-age stars. Such stars can overlap the RGB above its tip and near the RGB “edges” in luminosity and color. On the basis of artificial star trials we calculated the incompleteness levels for all studied fields, and corrected the measured stellar number density for this effect. In Figure 6, we present the results of completeness tests for two typical fields, S3 and S4. For M 81 we used red giants in magnitude range as follows: $24^m0 < I < 25^m0$ and $25^m5 < V < 26^m5$. From the mentioned above plots (Fig.6), we found that in case of field S3 sample completeness is 0.80 for I band and 0.35 for V band. In case of field S4, the completeness is 0.95 and 0.90, correspondingly. The AGB stars are more luminous than RGB ones and incompleteness correction is very small. To increase statistical significance of results, we estimated a mean number density of stars (AGB and RGB) for each of the three chips of WFPC2 (except small PC chip). The achieved results are presented in Figures 10 and 11. These figures demonstrate an apparent drop of stellar number density distribution. This drop corresponds to the outer edge of the thick disk. There are also a difference in surface number density gradients between RGB and AGB stars, increasing relative fraction of RGB over AGB stars towards increasing of galactocentric radius. The

radius of the M 81 thick disk have been estimated of $22'$ (see Fig. 11), which corresponds to 25 kpc. The available WFPC2 images do not reach the outer part of the M 81 stellar halo. The lower limit of the halo radius is ~ 40 kpc. A similar extended stellar halo have been detected in M 31 (Ferguson et al., 2002) and NGC5128 (Harris et al., 1999). Some of the fields around M 81's disk and halo are contaminated by the stellar populations of its dwarf satellite galaxies BK3N, Ho IX, and Arp's ring. It causes an excess of surface number density above the average level at given galactocentric radius (Figure 10).

The CMDs of satellite dwarf galaxies BK3N and Ho IX (Figure 10 and 11) show a presence of AGB stars, faint blue stars but lack of more evolved stellar populations (RGB stars), suggesting that BK3N and Ho IX might represent young tidal formations (Miller, 1995; Flynn et al., 1999; Boyce et al., 2001). The absence of RGB stars make it impossible to determine distances on the basis of TRGB method. The distance values obtained by Karachentsev et al. (2002) refer to halo and disk stars of M 81, but not to BK3N and Ho IX. At the same time, in the field of the Arp's ring both the AGB and RGB stars are apparent (Figure 10, and 11), providing a lower limit on its age, since RGB stars are at least a Gyr old. The detection of some blue stars in this field demonstrates the presence of low star formation in the ring.

4.6. NGC 300.

There are three WFPC2 fields in the HST archive, located nearly along the same galactocentric line, and six ACS/WFC fields (Figure 3). It is well seen (Fig. 12), that the thick disk and the halo demonstrate different gradient of star density decrease. As in the case of M81, the stellar surface density of the thick disk, can be well fit by exponential law (Figure 12). The thick disk of NGC 300 reveals a sharp edge, but it is impossible to determine the halo extend due to the lack of the HST data at larger galactocentric radius. As it is shown in Figure 12, the NGC 300 stellar halo spreads at least twice larger than thin disk. On the true-color picture of NGC 300 (MPG/ESO 2.2-m + WFI) a bluish disk with the sharp border on its outskirts can also be seen. All spiral arms are embedded into this disk. Usually size of such disks are considered as a visual size of the galaxy. Field S2 is situated on the edge of this bluish disk where all variations of stellar population can be studied. The number of blue stars (main sequence giants and supergiants) rapidly decreases on the edge of thin disk up to zero (see Fig.13). The number of AGB stars also decreases nearly to zero, but red giants of thick disk do not show a drop in the surface number density on the edge of thin disk and spread out of the thin disk borders. The thick-to-thin disk size ratio, however, is just ~ 1.2 (Figure 13).

4.7. NGC 55.

NGC 55 is edge-on galaxy and we can investigate its stellar density in the extraplanar Z-direction, i.e. perpendicular to the plane of the disk. From the analyzis of three fields, we determined the surface number density of the red giants in the range of extraplanar distances from 2 to 7 kpc (Figure 2). It was found that all the regions (S1, S2, S3) demonstrate the same gradient of the surface number density of the RGB stars, suggesting that all the fields are located in the thick disk. Surprisingly, despite of different galactocentric radii of the field S2 and S3 (Figure 2), both follow the same gradient of the RGB surface number density along the Z-direction. At the same time, the surface number density distribution do not show a sharp edge of the thick disk, and the possible presence of the at distance of at least >6 kpc is unclear (Figure 14). To determine the true extend of the thick disk and to reveal the halo, additional observations are necessary. In the lack of the fields on the different galactocentric distances (along the disk plane), we might estimate the radial extend of the thick disk from the mean axes (planar-to-extraplanar) ratio of $2.5 : 1$, obtained from our study of Irregular galaxies (Tikhonov, 2002). This give us a resulting galactocentric radius of the NGC 55 thick disk of ≈ 15 kpc.

Similar to M 81, the AGB stars of NGC 55 and NGC 300 show larger surface number density gradients, realtively to the RGB stars, and almost abscent in the galaxy outskirts. Due to their smaller statistics in the fields of NGC 55 and NGC 300, the derived surface number density gradients of the AGB stars are very uncertain for these galaxies.

5. Discussion.

On the basis of the study of star density in the three spiral galaxies, M 81, NGC 300 and NGC 55, we examine the spatial distribution of stars in a region of their thick disks and halos. The emphasis in the current work is on the extended surroundings of the galaxies, out to typically a few kpcs. The disks and halos of M 81 and NGC 300 have similar structure, but differ in spatial sizes. While thick disk in the NGC 55 is apparent, we found no significant evidence for a presence of stellar halo within 6 kpc of this galaxy.

A scaled 3-D model of the stellar structures of the typical spiral galaxy presented in Figure 15. The extraplanar size (thickness) of the thin disk depends from the galaxy type (Ma, 2002). A thickness of the thin disk in M81, NGC 55 and NGC 300 spans range of 0.7-1.5 kpc. The thick disk, as seen at NGC 55 (Fig.14), has thickness of 13 kpc, but the thick-to-thin disks size ratio is only $1.2 - 1.3$. The same ratio was observed in M 33 (Guillandre et al., 1998). By comparing a stellar structure of galaxies M 81 and NGC 300 with ones of irregular galaxies (Tikhonov, 2002) we noticed that while spiral galaxies have a small thick-to-thin disks size ratio, irregular galaxies demonstrate much larger ratio, from 2.5 to 5. A very large red giants disk was found in the dwarf lenticular galaxy NGC 404 (Tikhonov et al., 2003). It is plausible that all spiral galaxies

have not only a thick disk but also an extended halo, while dwarf irregular galaxies have only a thick disk. Knowing that bright irregular galaxy IC 10 has a thick disk and an extended halo (Drozdovsky et al., 2003), we suggest that in order to have the stellar halo a galaxy need to have the mass above the certain limit. Combining this work with results obtained for the spiral edge-on galaxies NGC 891, NGC 4144 and IC 5052 (Tikhonov et al. in preparation), we also suggest that their halo might be well represented by oblate ellipsoid (see Fig. 15). This elliptical shape have also the halo of spiral galaxy M 31 (Zucker et al., 2004). In order to come to statistically reliable conclusions, it is necessary to study stellar periphery of larger set of galaxies with different masses.

6. Summary.

It remains difficult to study outer stellar edges in the galaxies. However, the results presented here indicate that the pursuit of deep single-star photometry, followed by recovering the type of stars and their spatial distribution is meritorious for studying galactic outskirts. The star count method allows to trace extended surroundings of the galaxies, out to a few scale radii, much below the sensitivity of all other methods and constrain their spatial geometry with high confidence level.

On the basis of this method we have obtained the following major results:

- a) The extended stellar thick disks and halos have been detected in M 81, NGC 300 and NGC 55.
- b) There are clear differences between surface density gradients of the evolved stellar populations assigned to the thick disk and halo of these spiral galaxies, which allowed us to detect the edge of the thick disk.
- c) Having a large of dataset allowed us to estimate the distances to the galaxies from the TRGB method with high statistical confidence. We determine a distance of 3.85 ± 0.08 Mpc for M 81, 2.12 ± 0.10 Mpc for NGC 55, and 2.00 ± 0.13 Mpc for NGC 300, and a mean stellar metallicity of -0.65 , -1.25 , and -0.87 .
- d) There are clear differences in color distributions of the RGB stars, indicating plausible metallicity gradients in the thick disk and halo of the studied galaxies.

Large statistical studies of this kind are crucial for understanding the morphology of nearby galaxies. It is necessary to have a homogeneous dataset, obtained with the same equipment and uniformly analyzed. Datasets available on the HST/WFPC2/ACS Archive having deep homogeneous images with unparalleled resolution provide a unique way to analyze the physical characteristics of the shapes of galaxies with a high degree of confidence.

Our study would provide essential new input for theoretical models (as yet, our understanding of the three-dimensional structure of spirals is limited by central high-surface brightness disks), and may be relevant for the origin of dark matter in these galaxies,

as well as evolution of the galaxies. We view this archival study as part of a larger research project, involving followup ground based multiobject spectroscopy and wide-field imaging.

Acknowledgements. The authors would like to thank to the Russian Foundation for Basic Research for financial support under the grant 03-02-16344. Data from the NASA/IPAC Extragalactic Database have been used.

References

- Appleton P.N., Davies R.D., Stephenson R.J., 1981, MNRAS 195, 327
- Baggett W.E., Baggett S.M., Anderson K.S.J., 1998, AJ 116, 1626
- Barnes J.E. & Hernquist L., 1992, Nature 360, 715
- Bellazzini M., Cacciari C., Federici L., Fuci Pecci F., Rich M. , 2003, A&A 405, 867
- Boyce P. J., Minchin R. F., Kilborn V. A., Disney M. J., Lang R. H., Jordan C. A., Grossi M., Lyne A. G., Cohen R. J., Morison I. M., Phillipps S., 2001, ApJ 560L, 127
- Börngen F., Karachentseva V. E., Schmidt R., Richter G. M., Thaenert W., 1982, AN 303, 287
- Börngen F., Karachentseva V. E., Karachentsev I. D., 1984, AN 305, 53
- Bresolin F., Gieren W., Kudritzki R.-P., Pietrzynski G., Przybilla N., 2002, ApJ 567, 277
- Brewer M.-M., Carney B.W., 2004, PASA, 21, 134
- Brewer J., Richer H., Crabtree D., 1995, AJ 109, 2480
- Brown T.M., Ferguson H.C., Smith Ed., Kimble R.A., Sweigart A.V., Renzini A., Rich R.M., VandenBerg D. A., 2003, ApJ 592, L1
- Bullock J.S., Kravtsov A.V., Weiberg D.H., 2001, ApJ 548 ,33
- Burkert A., Truran J. W., Hensler G., 1992, ApJ 391, 651
- Butler D. J., Martínez-Delgado, D. and Brandner, W., 2004, AJ 127, 1472
- Byun Y.I. & Freeman K.C., 1995, ApJ 448, 563
- Caldwell N., Armandroff T.E., Da Costa G.S., Seitzer P., 1998, AJ 115, 535
- Carney B.W., Latham D.W., & Laird J.B., 1989, AJ 97, 423
- Chiba M. & Beers T.C., 2000, AJ 119, 2843
- Cote S., Freeman K., Carignan C., Quinn P., 1997, AJ 114, 1313
- Dalcanton J.J. & Bernstein R.A., 2002, AJ 124, 1328
- Deeg H.J., Munoz-Tunon C., Tenorio-Tagle G., Telles E., Vilchez J. M., Rodriguez-Espinosa J. M., Duc P. A., Mirabel I. F., 1998, A&AS 129, 455
- Drozdovsky I., Tikhonov N., Schulte-Ladbeck R., "The outer stellar edges of irregular galaxies: IC10 and LeoA", 2003, STScI May 2003 Symposium
- Drozdovsky I., Schulte-Ladbeck R., Tikhonov N., "The outer edges of dwarf irregular galaxies: stars and gas", 10-11 October, 2002, Lowell Workshop
- Duc P.-A., Mirabel I.F., 1998, A&A 333, 813
- Eggen O.J., Lynden-Bell D. & Sandage A.R., 1962, ApJ 136, 748
- Elmegreen B.G., Kaufman M., Thomasson M., 1993, ApJ 412, 90
- Engelbracht C. W., MIPS Science Team, SINGS Team, 2004, AAS 204, 3311
- Ferguson A. M. N. & Johnson R.A., 2001, ApJ 559L, 13

- Ferguson A. M. N., Irein M. J., Ibata R.A., Lewis G.F., Tanvir N. R., 2002, *AJ* 124, 1452
- Friel E.D. & Janes A., 1993, *A&A* 267, 75
- Flynn L., Walterlos R.A.M., Thilker D.A., Fierro V., 1999, 5-9 January, AAS Meeting 193 - Austin, Texas
- Freedman W.L., Madore B.F., Hawley, S. L.; Horowitz I. K., Mould J., Navarrete M., Sallmen S., 1992, *ApJ* 396, 80
- Freedman W.L., Hughes S.M., Madore B.F., 1994, *ApJ* 427, 628
- Freedman W.L., Madore B. F., Gibson B. K., Ferrarese L., et al. 2001, *ApJ* 553, 47
- Georgiev Ts. B., Bilkina B.I., Tikhonov N.A., 1992, *A&AS* 95, 581
- Georgiev Ts. B., Bilkina B.I., Tikhonov N.A., 1992, *A&AS* 96, 569
- Gilmore G., & Wyse R.F.G., 1985, *AJ* 90, 2015
- Gilmore G., Wyse R.F.G., & Norris J., 2002, *ApJ* 574, L39
- Graham J.A., 1982, *ApJ* 252, 474
- Graham J.A., 1984, *AJ* 89, 1332
- Guillandre J., Lequeux J., Loinard L., 1998 in *IAU Symp. 192, The Stellar content of Local Group Galaxies*, ed. Whitelock P., Cannon R., 27
- Harris W.E. & Harris G. L. H., 2001, *AJ* 122, 3065
- Harris G., Harris W., Poole G., 1999, *AJ* 117, 855
- Holtzmann J.A., Hester J.J., Casertano S., 1995a, *PASP* 107, 156
- Holtzmann J.A., Burrows C.J., Casertano S., Hester J.J., Trauger J.T., Watson A.M., & Worthey G., 1995b, *PASP* 107, 1065
- Hunsberger S.D., Chareton J.C., Zaritsky D., 1996, *ApJ* 462, 50
- Harris W. E., Harris G.L.H., 2001, *AJ* 122, 3065
- Jerjen H., Binggeli B., Freeman K., 2000, *AJ* 119, 593
- Ibata R.A., Gilmore G., Irwin M.J., 1995, *MNRAS* 277, 781
- Karachentsev I. D., Dolphin A. E., Geisler D., Grebel E. K., Guhathakurta P., Hodge P. W., Karachentseva V. E., Sarajedini A., Seitzer P., Sharina M. E., 2002, *A&A* 383, 125
- Karachentseva V. E., Karachentsev I. D., Boerngen F., 1985, *A&AS* 60, 213
- Kent S.M., 1985, *ApJS* 59, 115
- Kim M., Kim E., Lee M. G., Sarajedini A., Geisler D., 2002, *AJ* 123, 244
- Kiszkurno-Koziej E., 1988, *A&A* 196, 26
- Lee M.G., Freedman W.L., Madore B.F., 1993, *AJ* 417, 553
- Lee M.G., Kim M., Sarajedini A., Geisler D., Gieren W., 2002, *ApJ* 565, 959
- Ma J., 2002, *A&A* 388, 389
- Geisler D., 2000, *AJ* 119, 760
- Makarova L. N., Grebel E. K., Karachentsev I. D., Dolphin A. E., Karachentseva V. E., Sharina M. E., Geisler D., Guhathakurta P., Hodge P. W., Sarajedini A., Seitzer P., 2002, *A&A* 396, 473
- Marquez I., Masegosa J., Moles M., Varela J., Bettoni D., Galletta G., 2002, *A&A*, 393, 389
- Miller B.W., 1995, *BAAS* 185, 1365
- Oshima T., Mitsuda K., Ota N., Yamasaki N., 2002, *The 8th IAU Asian-Pacific Regional Meeting, July 2-5, 2002, Tokyo, Japan*, 287

- Otte B. & Dettmar R.-J., 1999, A&A 343, 705O
- Pierre M. & Azzopardi M., 1988, A&A 189, 27
- Prieto M., Aguerri J. A. L., Varela A. M., Munoz-Tunon C., 2001, A&A 367, 405
- Pritchett C. J., Schade D., Richer H. B., Crabtree D., Yee H. K. C. 1987, ApJ 323, 79
- Pritchett C.J. and van den Bergh S., 1988, ApJ 331, 135
- Prochaska J.X., Naumov S. O., Carney B. W., McWilliam A., Wolfe A. M., 2000, AJ 120, 2513
- Puche D., Carignan C., Bosma A., 1990, AJ 100, 1468
- Puche D., Carignan C., Wainscoat R. J., 1991, AJ 101, 447
- Reitzel D.B. & Guhathakurta P., 2002, AJ 124, 234
- Rogstad D.H., Crutcher R.M. and Chu K., 1979, ApJ 229,509
- Rolleston W.R.J., Smart S.J., Dufton P.L., Ryans R.S.I., 2000, A&A 363, 537
- Sakai S. & Madore B., 2001, ApJ 555, 280
- Sarajedini A., Geisler D., Schommer R., Harding P., 2000, AJ 120, 2437
- Sarajedini A. & Van Duyne J., 2001, AJ 122, 2444
- Searle L., Zinn R., 1978, ApJ 225,357
- Shaver P.A., McGee R.X., Danks A.C., Pottasch S.R., 1983, MNRAS 204, 53
- Schlegel D. J., Finkbeiner D.P.; Davis M., 1998, ApJ 500, 525
- Stetson, P.B. 1994, Users Manual for DAOPHOT II
- Tenjes P., Haud U., Einasto J., 1998, A&A 335, 449
- Tikhonov N.A., 1999, IAUS, 192, 244
- Tikhonov N.A., 2002, Dissertation, St-Petersburg State University, Russia
- Tikhonov N.A., Galazutdinova O.A., Aparicio A., 2003, A&A 401, 863
- Vallenari A., Bertelli G., Schmidtbreick L., 2000, A&A 361, 73
- Venn K.A., Irwin M., Shetrone M.D., Tout C.A., Hill V., Tolstoy E., astro-ph/0406120
- van der Hulst J.N., 1978, in Structure and Properties of Nearby Galaxies, IAU Symp., No.77, (Reidel, Dordrecht and Boston), 269
- van der Marel R.P. 2001, astro-ph/0107248
- Weilbacher P.M., 2002, PhD Dissertation, Notingen
- Westpfahl D. J., Coleman P. H., Alexander J., Tongue T., 1999, AJ 117, 868
- Williams B.F., 2002, MNRAS 331, 293
- Yun M.S., Ho P.T.P., Lo K.Y., 1994, Nature 372, 530
- Zickgraf F.-J., Humphreys R. M., Sitko M. L., Manley T., 1990, PASP 102, 925
- Zoccali M., Renzini A., Ortolani S., Greggio L., Saviane I. , Cassisi S., Rejkuba M. , Barbuy B., Rich R.M., Bica E., 2002, astro-ph/0210660
- Zucker D.B., Kniazev A.Y., Bell E.F., Martinez-Delgado D., Grebel E.K., Rix H.-W., Rockosi C.M., Holtzman J.A., Walterbos R.A.M., Ivezić Z., Brinkmann J., Brewington H., Harvanek M., Kleinman S.J., Krzesinski J., Long D., Newman P.R., Nitta A., Snedden S.A., 2004, astro-ph/0401098

Table 1. Properties of NGC 55, NGC 300, M 81 (from NED).

Galaxy	NGC 55	NGC 300	M 81
RA (J2000)	$00^h 14^m 54^s$	$00^h 54^m 54^s$	$09^h 55^m 33^s$
DEC (J2000)	$-39^\circ 11' 49''$	$-37^\circ 41' 00''$	$69^\circ 03' 55''$
Morphological type	SB(s)m:sp	SA(s)d	SA(s)ab:LINER Sy1.8
Helio radial velocity (km/s)	129 ± 3	144 ± 1	-34 ± 4
Diameter (arcmin)	32.4×5.6	21.9×15.5	26.9×14.1
Magnitude	$8^m 84$	$8^m 95$	$7^m 89$
A_V	$0^m 044$	$0^m 042$	$0^m 266$
A_I	$0^m 026$	$0^m 025$	$0^m 155$
Inclination	85°	40°	59°

The Galactic extinction correction by Schlegel et al.(1998).

The inclination taken from LEDA.

Table 2. Observational log of HST.

Galaxy	Region	Date	Band	R	Exposure	ID	N _{stars}
M 81	S1	17.04.1998	F814w	2.96	1000+1200	7909	18164
			F606w	2.96	2×1000	7909	
	S2	26.01.1999	F814w	5.18	3×1500	8059	22933
			F606w	5.18	5×1500	8059	
	S3	4.06.2001	F814w	3.47	4×500	9073	19143
			F555w	3.47	4×500	9073	
	S4	30.06.2001	F814w	12.78	3×1400	9086	1611
			F606w	12.78	4×1300	9086	
	S5	1.09.2001	F814w	6.09	2×1100	8584	10150
			F555w	6.09	2×1100	8584	
	S6	28.05.2002	F814w	9.52	800	9634	7810
			F606w	9.52	2×500	9634	
	BK3N	29.08.2000	F814w	10.87	600	8061	519
			F606w	10.87	600	8061	
	Ho IX	27.06.2001	F814w	11.39	600	8061	3655
			F606w	11.39	600	8061	
NGC 300	Arp's loop	30.07.2000	F814w	17.61	600	8061	956
			F606w	17.61	600	8061	
	S1	13.09.2001	F814w	7.12	2×500	8584	4387
			F555w	7.12	2×500	8584	
	S2	02.07.2001	F814w	5.99	2×300	9162	12004
			F606w	5.99	2×300	9162	
	S3	20.06.2001	F814w	12.83	4×500	9086	2520
			F606w	12.83	4×500	9086	
	F1	17.07.2002	F555w	8.05	1080	9492	89615
			F814w	8.05	1080	9492	
	F2	19.07.2002	F555w	2.07	1080	9492	182106
			F814w	2.07	1080	9492	
	F3	28.09.2002	F555w	0.91	1080	9492	191107
			F814w	0.91	1080	9492	
	F4	21.07.2002	F555w	8.97	1080	9492	53494
			F814w	8.97	1080	9492	
NGC 55	F5	25.12.2002	F555w	5.45	1080	9492	128370
			F814w	5.45	1080	9492	
	F6	26.09.2002	F555w	6.15	1080	9492	68730
			F814w	6.15	1080	9492	
	S1	13.06.2001	F814w	8.00	4×500	9086	832
			F606w	8.00	4×500	9086	
	S2	15.06.2000	F814w	3.59	2×800+900	8697	5654
			F555w	3.59	3×800	8697	
	S3	10.06.2000	F814w	8.97	2×800+900	8697	10532

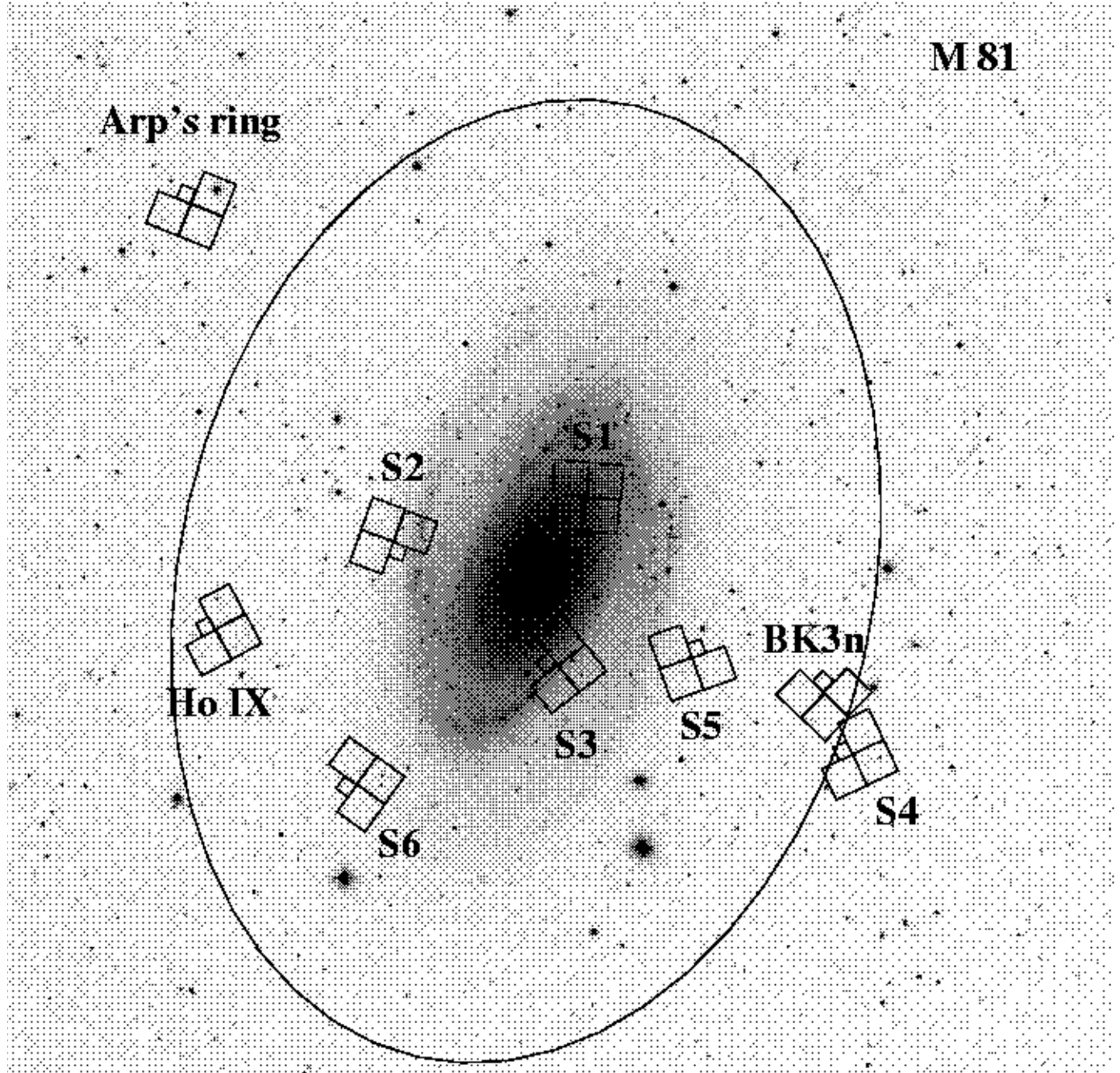


Fig. 1. DSS-2 $40' \times 40'$ image of M 81 with HST/WFPC2 footprints superposed, indicating 9 regions (S1, S2, S3, S4, S5, S6, BK3N, Ho IX, Arp' ring) observed. The edge of thick disk of red giants is marked by ellipse.

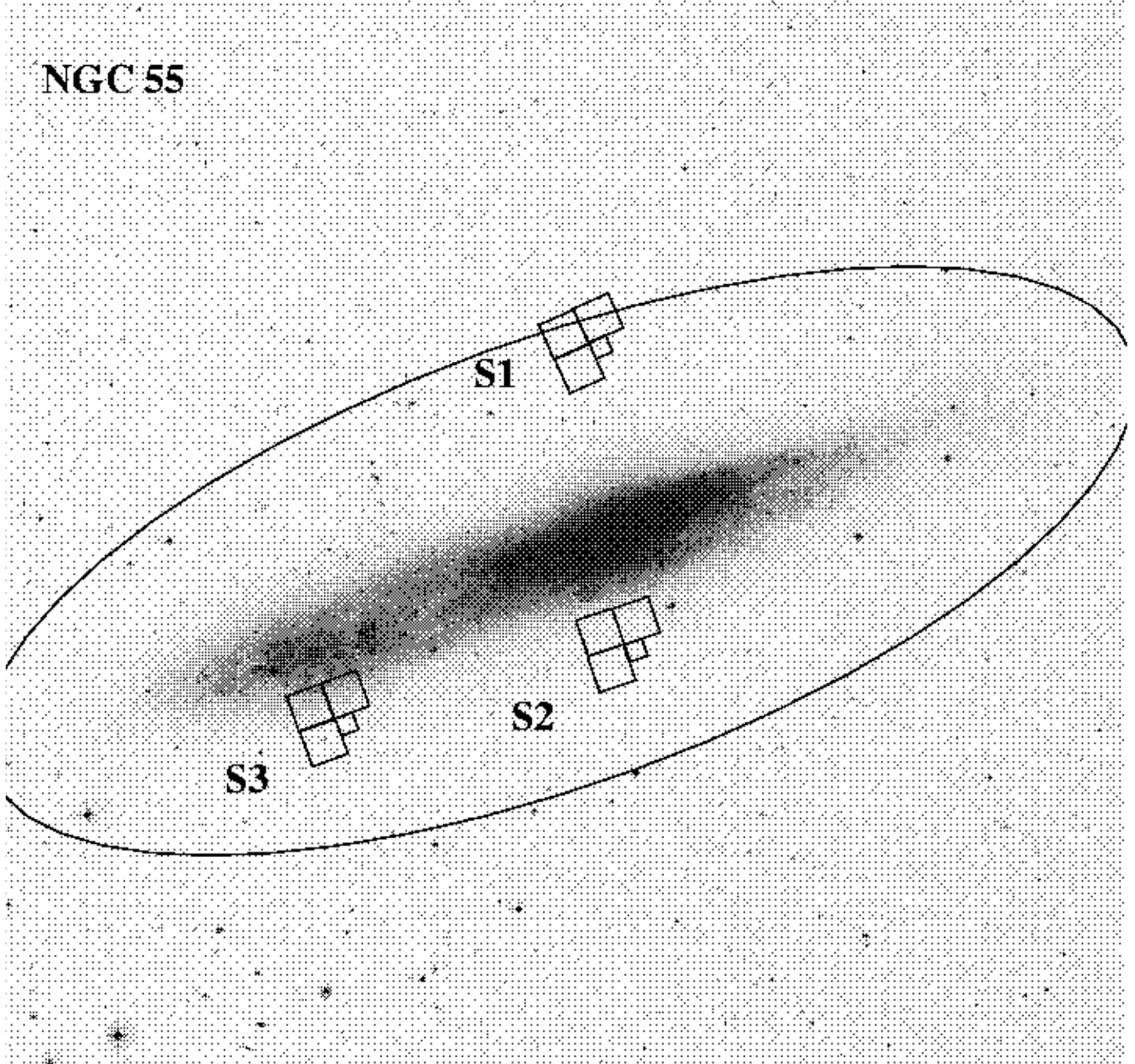


Fig. 2. DSS-2 $40' \times 40'$ image of NGC 55. The location of the HST/WFPC2 fields (S1, S2, S3) is indicated. The edge of thick disk of red giants is shown by ellipse.

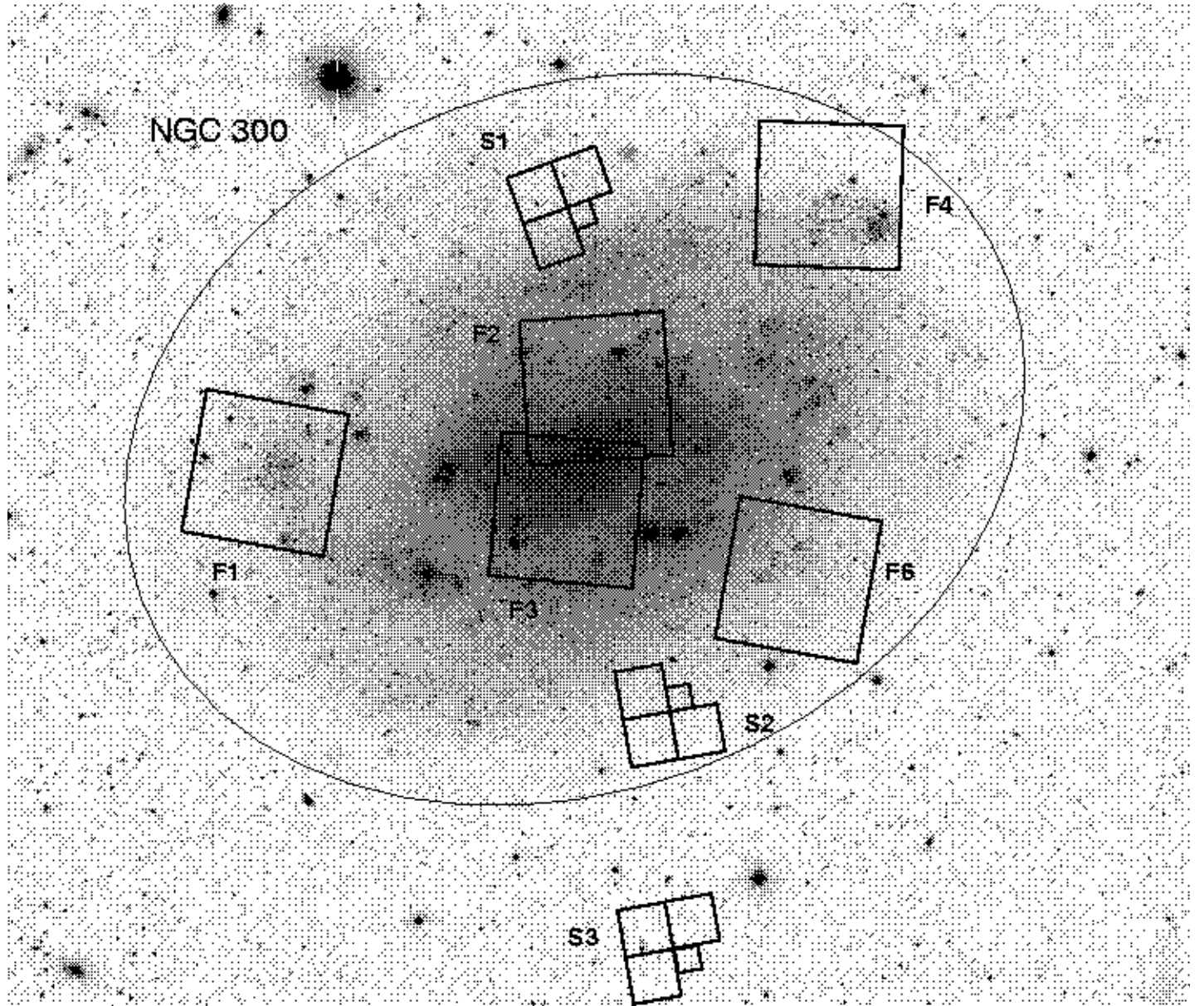


Fig. 3. $34' \times 33'$ WFI image of NGC 300 obtained with the MPG/ESO 2.2m telescope. The WFPC2 and ACS/WFI footprints are indicating 9 studied fields: S1, S2, S3, F1, F2, F3, F4, F5, F6). The edge of the stellar thick disk is marked by ellipse.

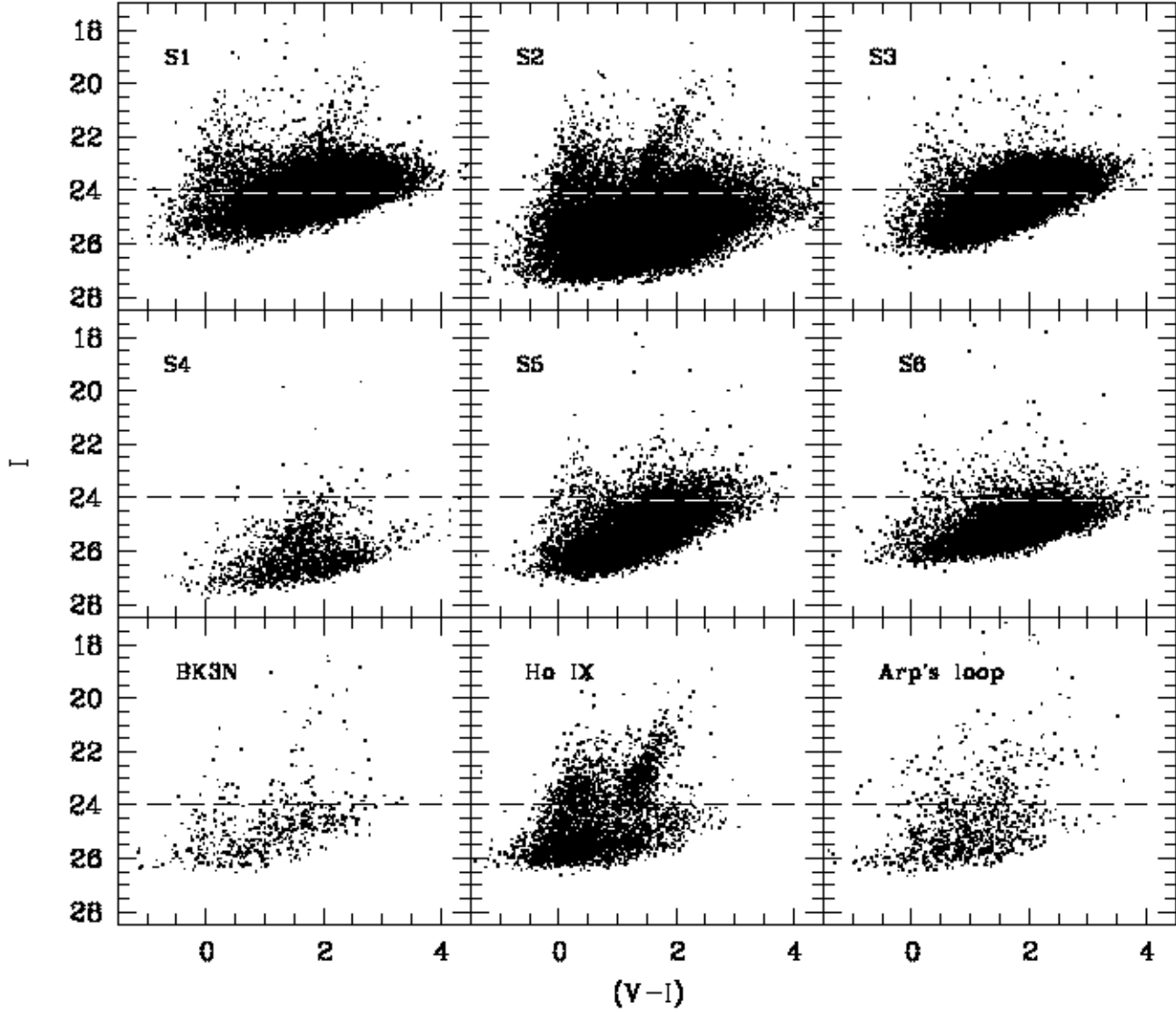


Fig. 4. $[(V - I), I]$ Color-Magnitude diagrams of different fields of M 81. The dashed line shows the position of the TRGB. Spatial variations in the stellar content are immediately apparent from the varying strengths of the blue and red plumes.

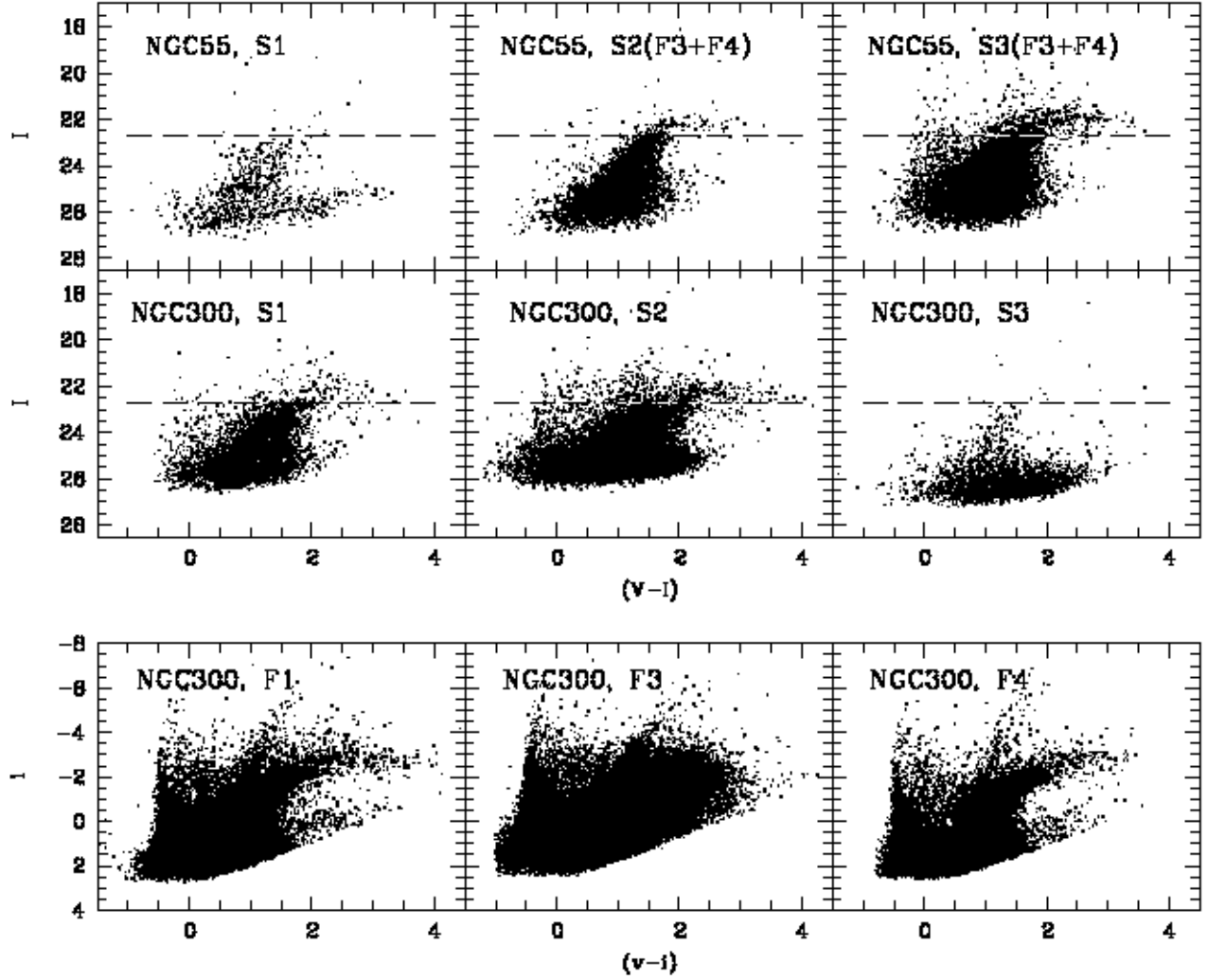


Fig. 5. *Top.* The $[(V-I), I]$ CMDs of different WFPC2 fields of NGC 55 and NGC 300. The dashed line shows the position of the TRGB. *Bottom panels* show the ACS/WFC CMDs of NGC 300 in the HST Vegamag system.

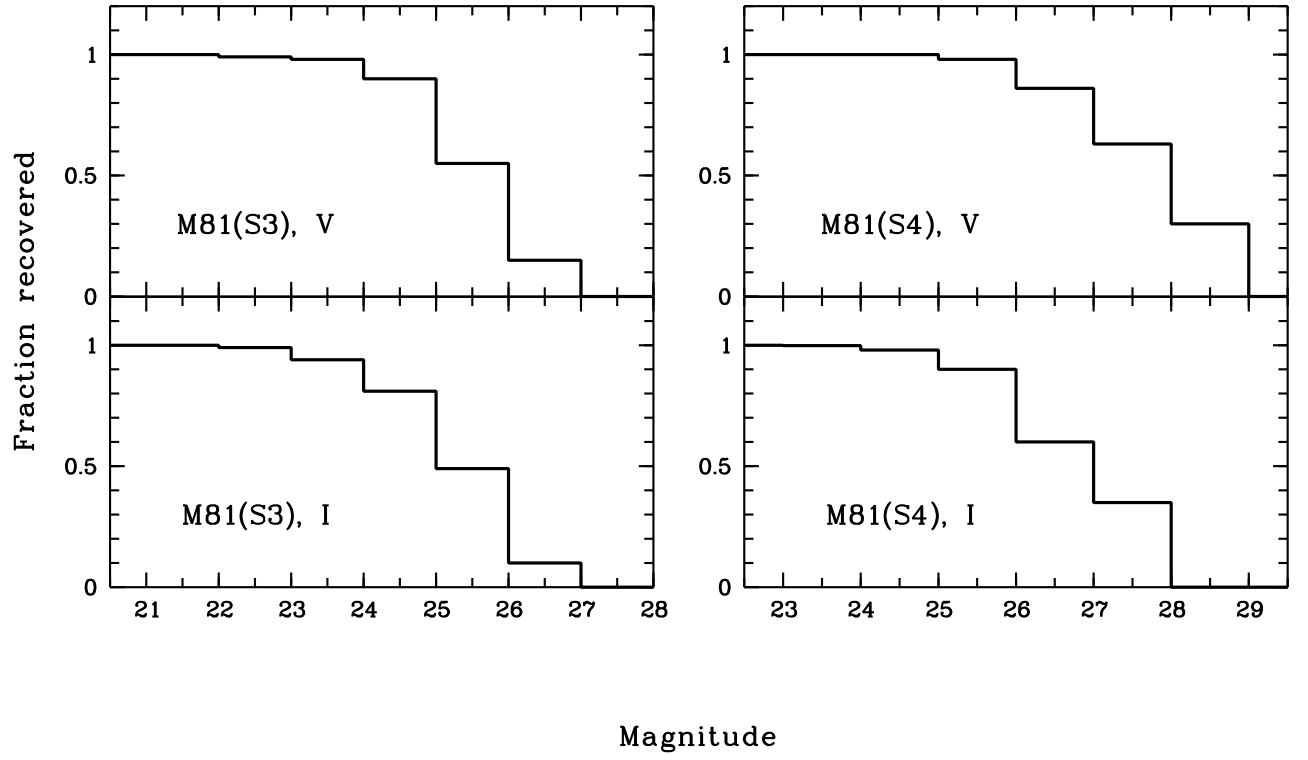


Fig. 6. Completeness levels of the WFPC2 photometry of the M 81 (S3 and S4 regions) based on artificial star test.

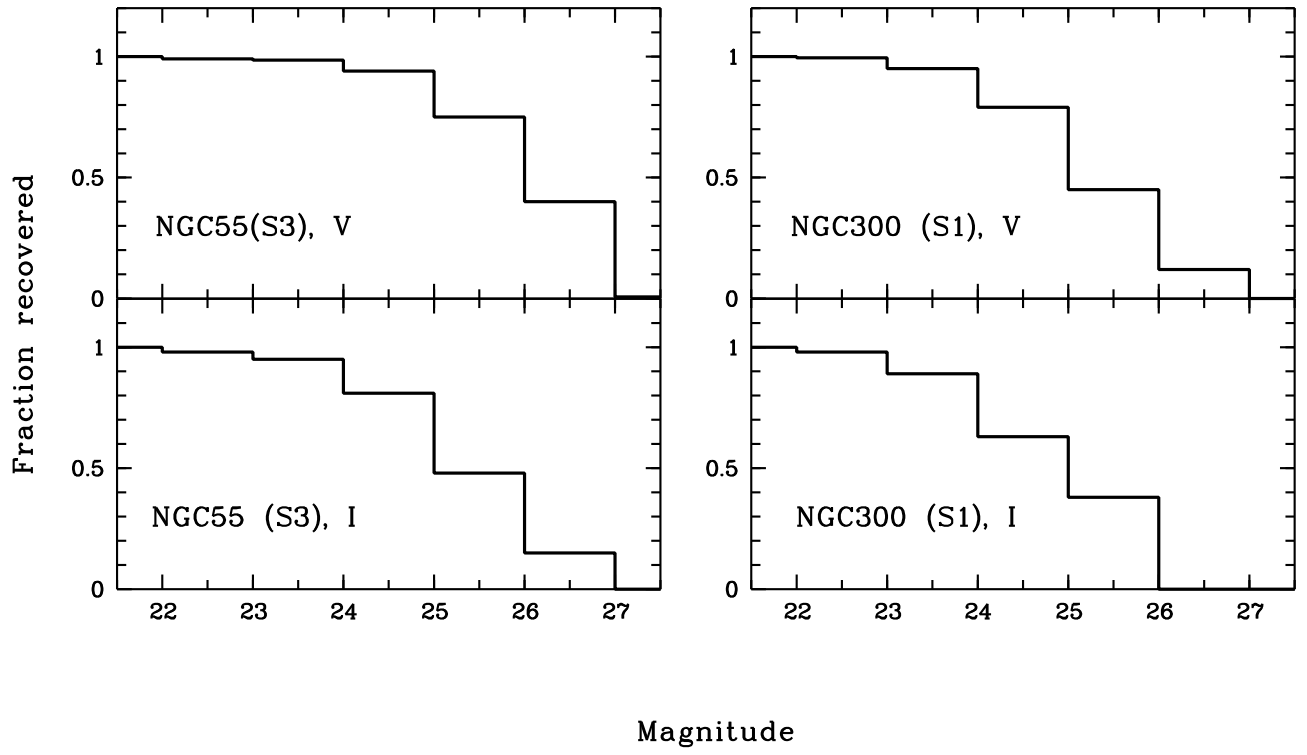


Fig. 7. Completeness levels for NGC 55 (Field S3) and NGC 300 (Field S1).

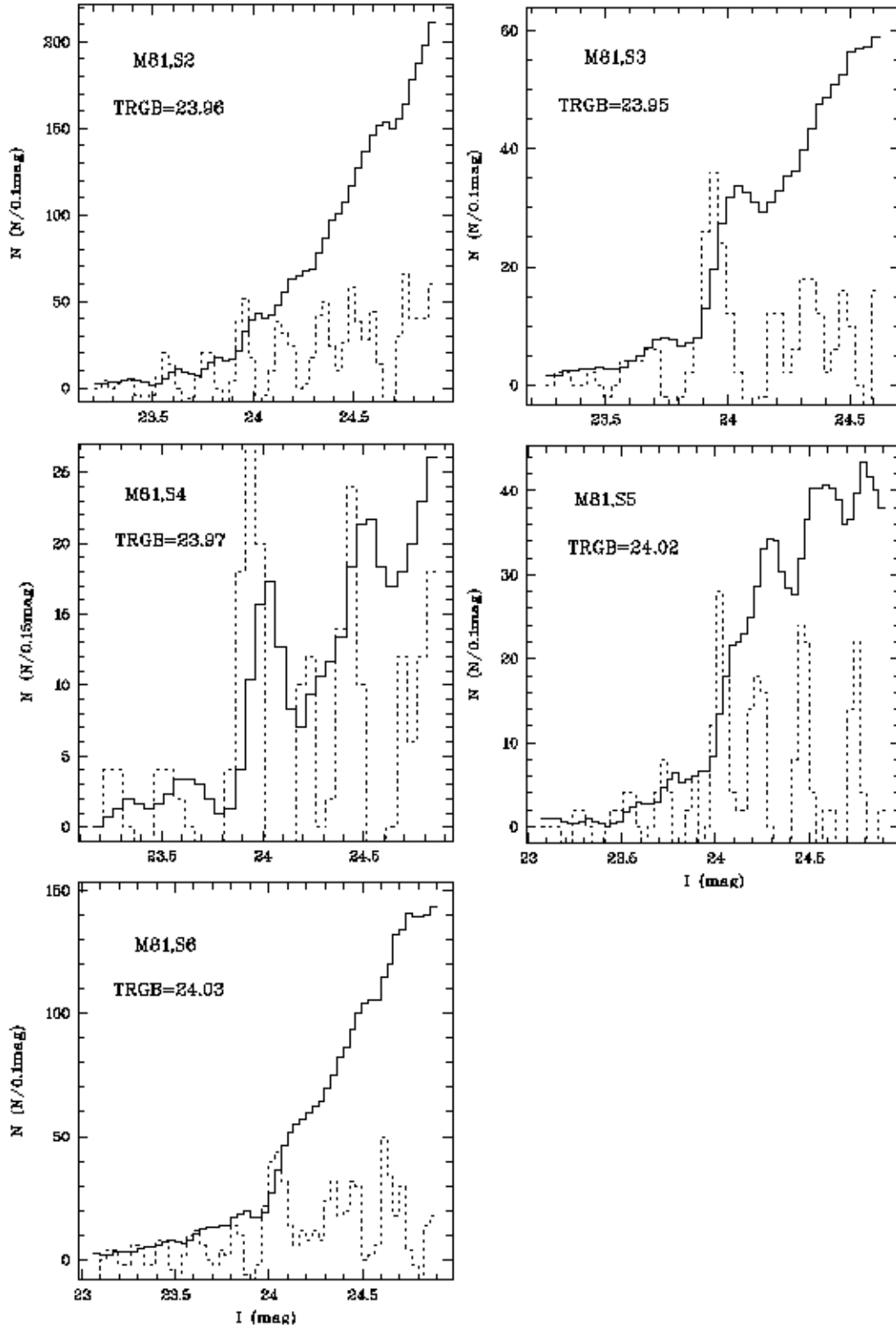


Fig. 8. Smoothed luminosity function LF (solid lines) and edge-detection Sobel-filter output (dotted lines) for different fields of M81. The position of the TRGB corresponds to the peak of the Sobel-filter.

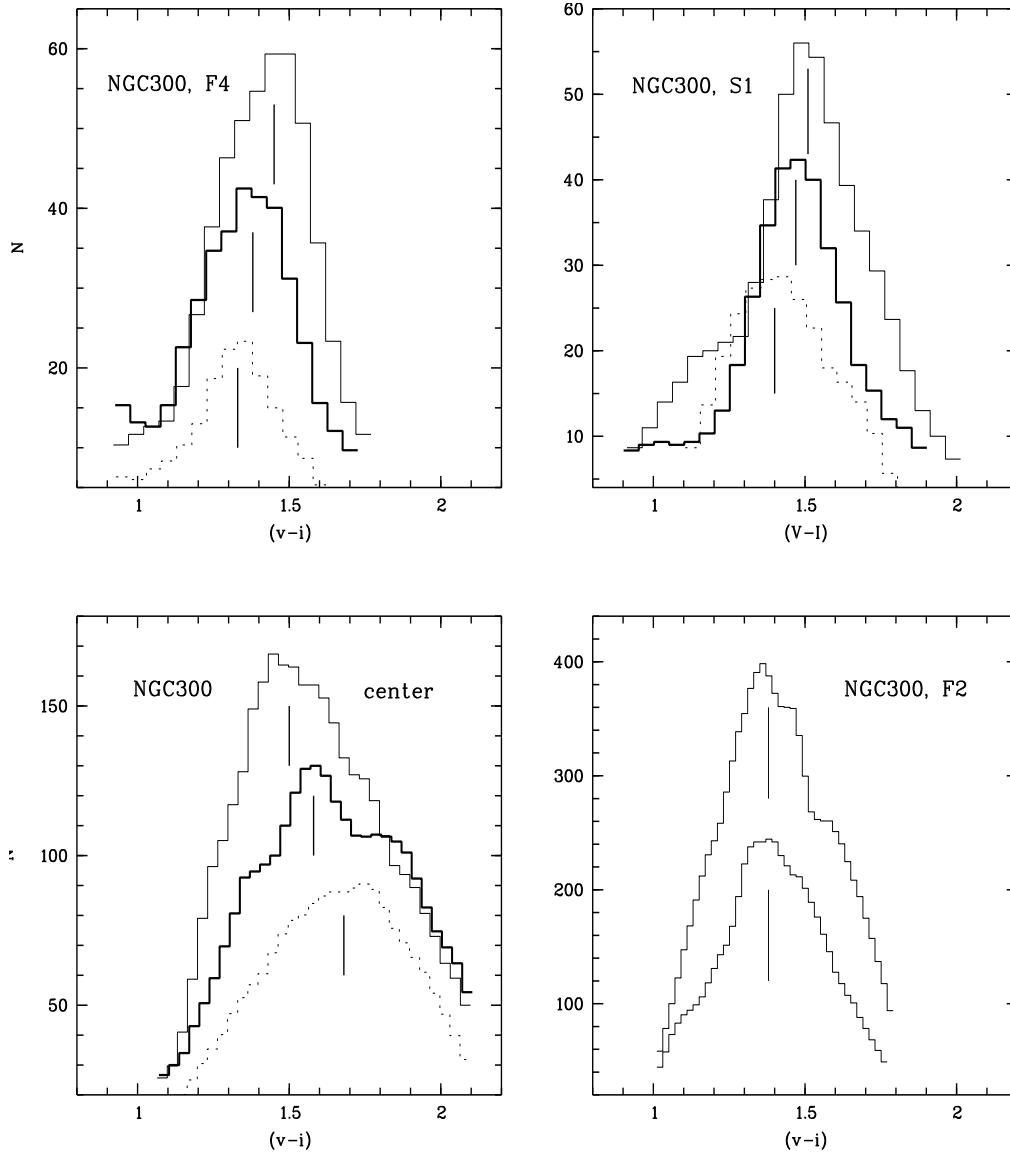


Fig. 9. The distribution of the $(V - I)$ (for WFPC2 data) and Vegamag $(v - i)$ (ACS/WFC) color of the RGB stars from 0.3 to 0.7 magnitudes below the tip of the RGB along the galactocentric radius for the different fields of NGC 300. Fields F4 and S1 are located at the edge of the galaxy thick disk, field F3 are near the galaxy center and field F2 is situated in the main galaxy body. The outer fields clearly demonstrate a systematic color shift along galactocentric radius. In the center field F3 the decrease in color of RGB might be due to effect of age, metallicity and redenning. The results for the main body field F2, do not show a change of RGB color along the galactocentric radius. The dashed line corresponds to a more distant part of the chip.

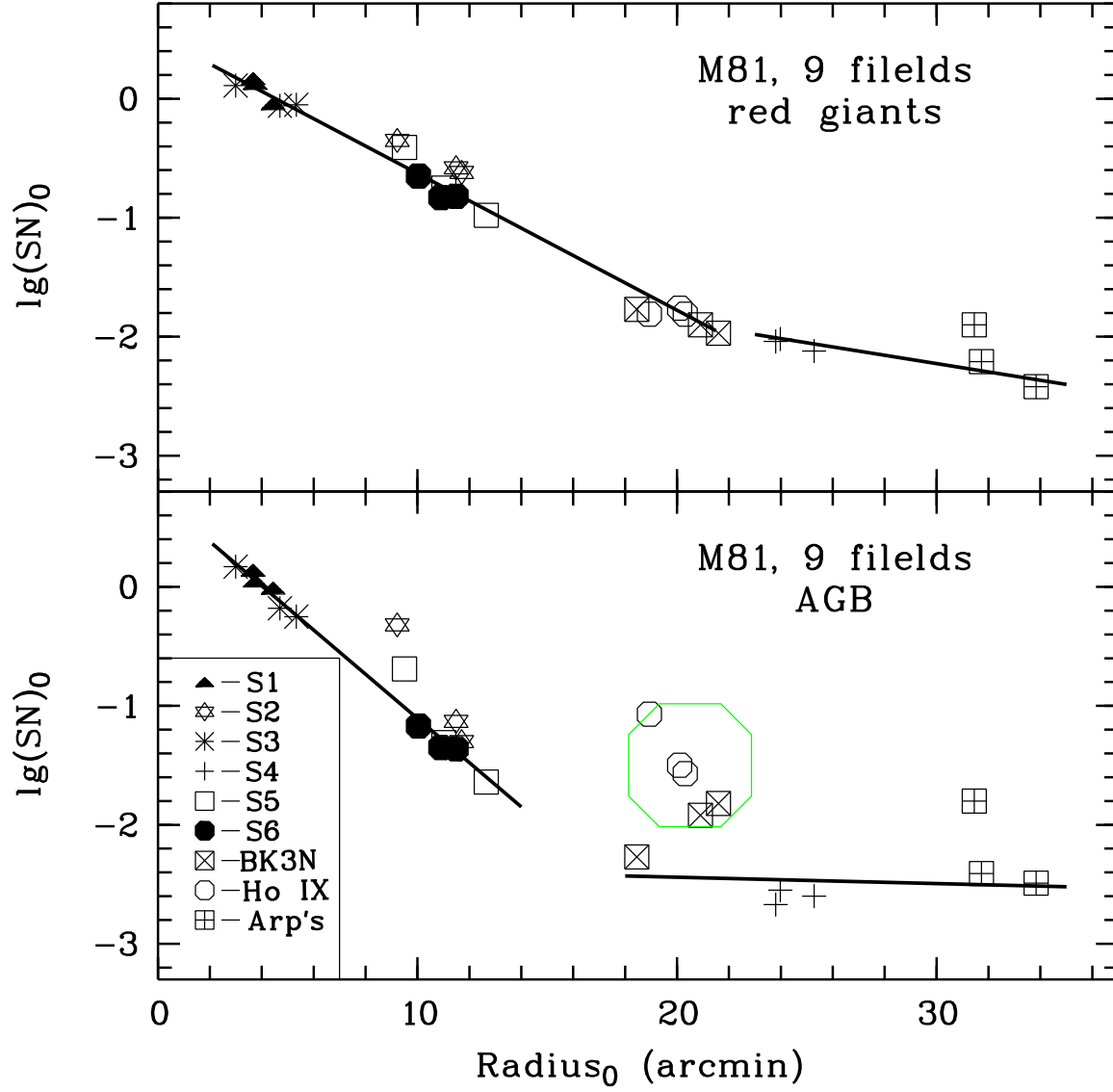


Fig. 10. The surface density distribution of RGB (top) and AGB (bottom) stars, $(SN)_0$, along galactocentric radius of M 81, corrected for the inclination. Star counts have been corrected for the incompleteness based on the artificial star trials. The absence of data for $13' < Radius_0 < 18'$ is due to insufficient images in these regions. The deviation of some points from the average level of the stellar density is a result of the combination of M 81 disk/halo evolved stars with the stars of its satellites BK3N, Ho IX, and Arp's ring.

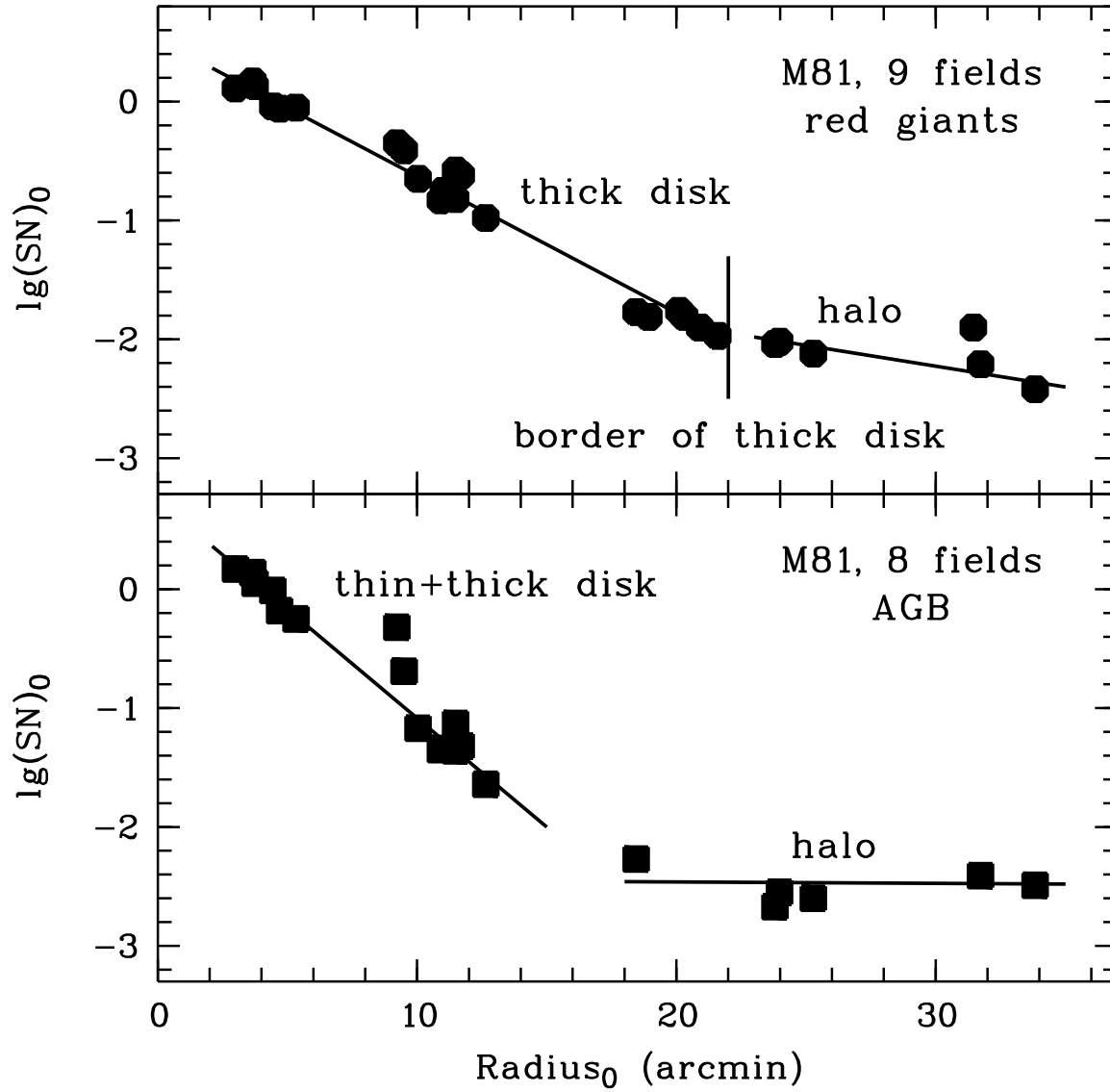


Fig. 11. Similar to Fig. 10, the distribution of RGB (top) and AGB (bottom) stars, but areas around the dwarf satellite galaxies is excluded. This allow us to determine the edge of the thick disk. The difference in gradients of AGB and RGB stars surface density is apparent.

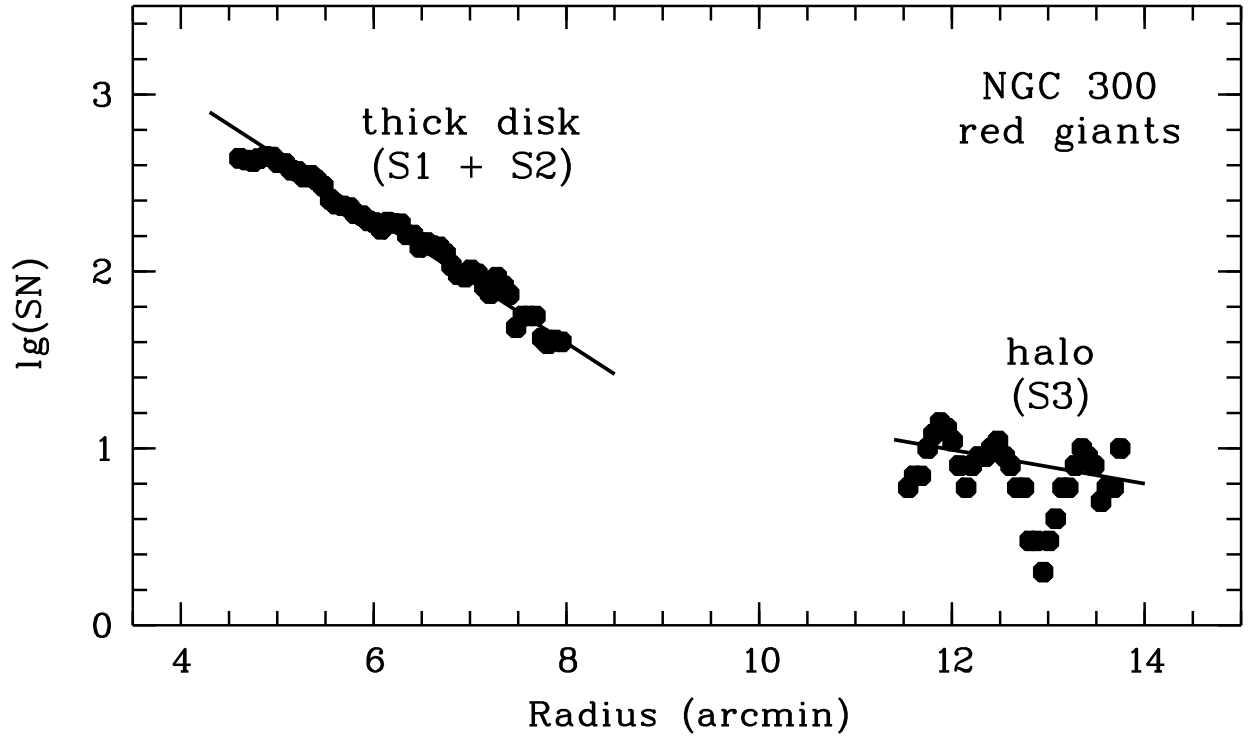


Fig. 12. The surface density distribution (SN) of RGB stars along the galactocentric radius. Similarly to M 81, the stellar density distribution suggests two different gradients, which we attribute to the thick disk and halo components.

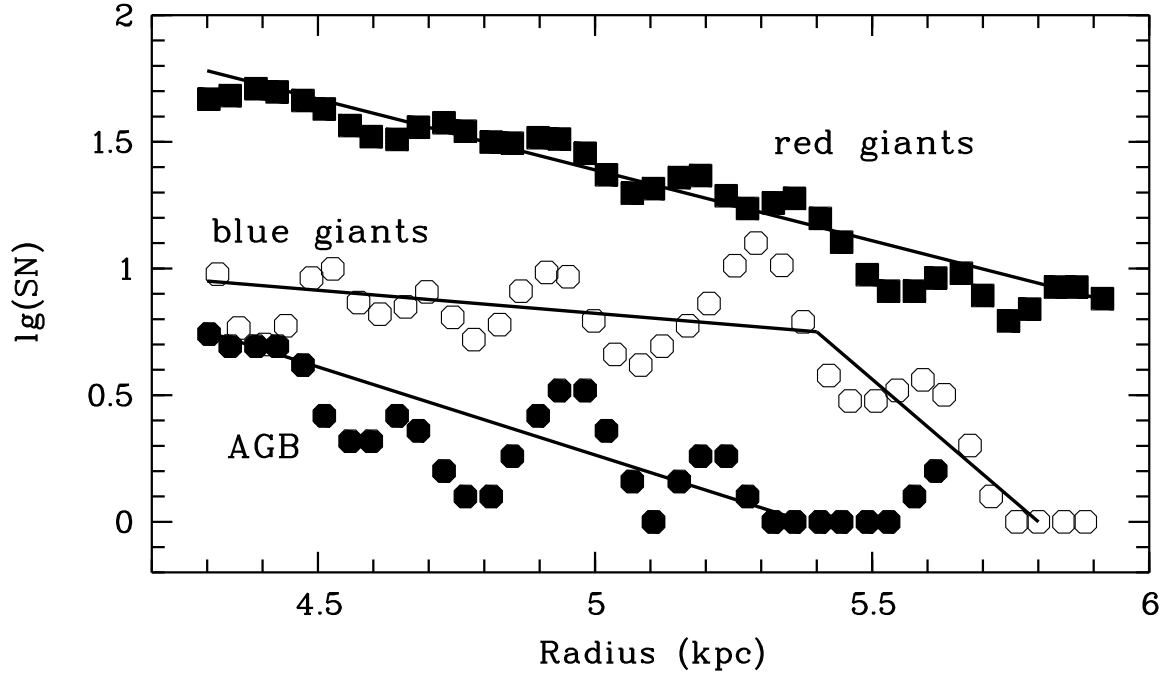


Fig. 13. The surface density distribution of RGB, AGB and blue stars in the edge of thin disk of NGC 300 (field S2). The drop in the surface number density of blue stars at the galactocentric radius of 5.7 kpc suggests that we reach the edge of thin disk. The red giants of the thick disk extend to a larger radii. Additional observations targeted at studying parts with larger galactocentric distances are necessary to determine the true size of the stellar thick disk/halo at this galaxy.

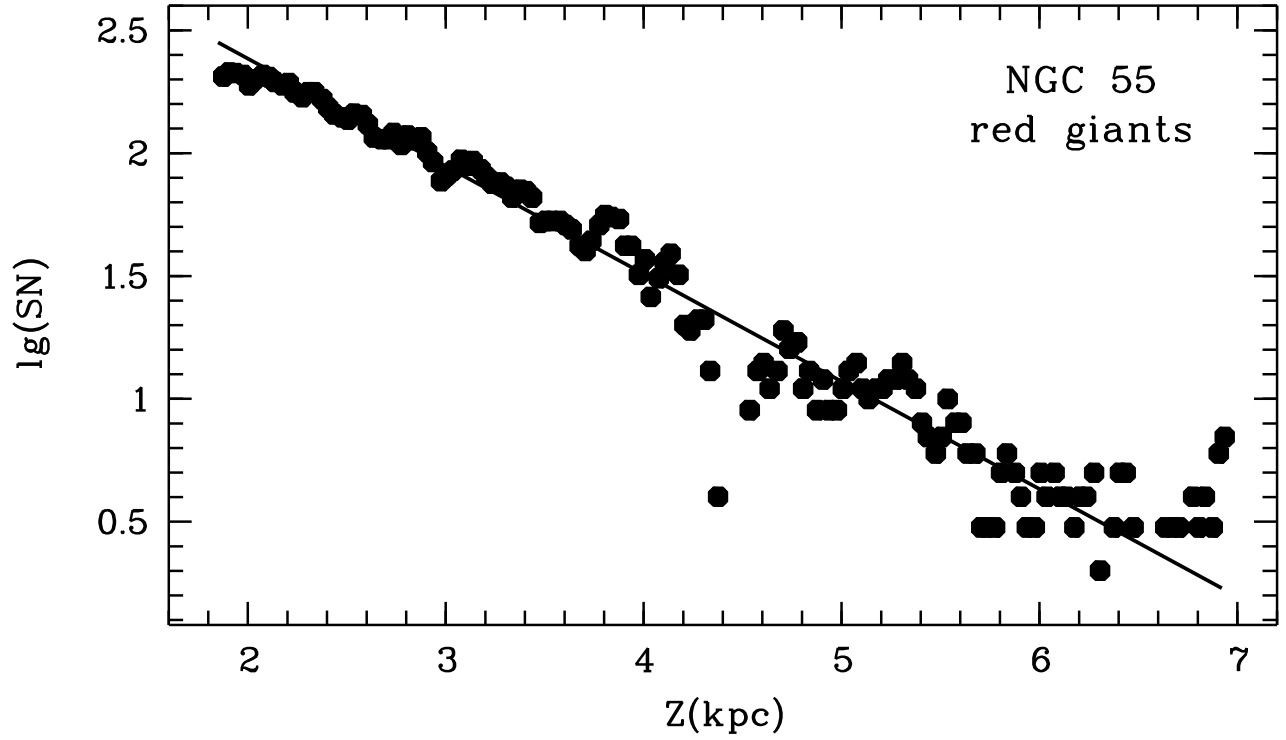


Fig. 14. The surface density distribution of RGB stars in NGC 55 (S1, S2, S3 fields) perpendicular to the galactic plane. The thick disk component is dominant with possible trace of the halo can be seen out of $Z > 6$ kpc.

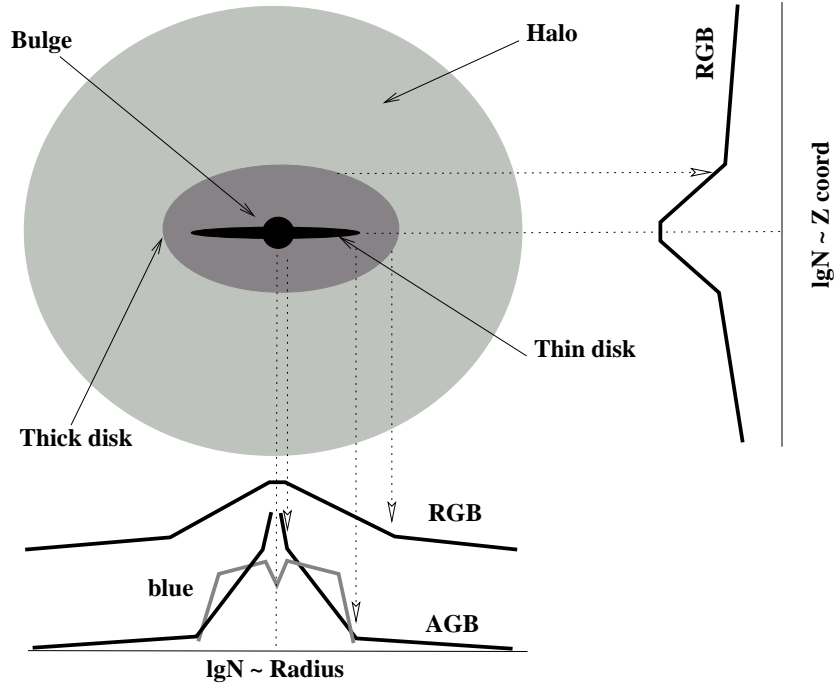


Fig. 15. A scaled 3-D representation of the stellar components of a typical spiral galaxy and results of their projection as a stellar number density for a face-on (bottom plot) and edge-on (right) galaxy. The thickness of the thin disk is from Ma, 2002. The relative sizes of thick to thin disks are from our investigations of M81, NGC300. This results is also in agreement with M 33 by Guilandre, 1998. The relative size of stellar halo in M 81 and NGC 300 is shown as a lower limit.